Key Engineering Materials Vols. 127-131 (1997) pp 961-968

doi:10.4028/www.scientific.net/KEM.127-131.961

Structure and Texture Evolution of the Metal Matrix Composite PM2014 Al-20%Al_2O_3 during Superplastic Deformation

R. Kaibyshev and V. Kazyhanov

Institute for Metals Superplasticity Problems RAS, Khalturina 39, Ufa, 450001, Russia

Keywords: Metal Matrix Composite, Superplasticity, Texture, Grain Boundary Sliding

ABSTRACT

Grain structure and texture evolution during superplastic deformation were studied on the PM2014-20%Al_2O_3 metal matrix composite produced via a powder technology method. Samples were deformed in tension at different strains in the range of true strain rates 10^{-4}-10^{0} s^{-1} at temperature T=500^{0}C. It was shown that in the initial stage of superplastic flow deformation bands are formed in the aluminum matrix along the tension direction. Initial <111> fibre texture is broken and formation of <110> fibre texture takes place. Further strain up to ε=50% leads to dynamic recrystallization occurrence inside the deformation bands. This yields the formation of a fine-grained structure. The <111> fibre texture is restored. Both at low strain rates in region I and at high strain rates in region III no microstructural band formation is observed and <111> fibre texture is retained during plastic deformation. These experimental results are caused by the fact that a character of cooperative grain boundary sliding (CGBS) is strain rate dependent. Examination of surface shows that in region II the CGBS is highly non-uniform while at lower and higher strain rates grain boundary sliding is much more homogeneous. The effect of reinforcements on uniformity of CGBS and, consequently, on structure and texture evolution is discussed.

1. INTRODUCTION.

It is known, that discontinuously reinforced metal matrix composites (MMC) exhibit superplastic behavior at relatively high strain rates ($\dot{\varepsilon}\geq10^{-2}$ s^{-1}) [1]. The optimum strain rate range for superplastic deformation (SPD) is from two to four orders of magnitude larger than that for monolithic aluminum alloys [1-3]. The superplastic deformation behavior of numerous MMCs has been well investigated [4]. However, these works have focused on mechanical properties. At the same time, the structure and texture evolution during superplastic flow has not been studied. Another unknown aspect of high strain rate superplasticity (HSRS) in MMCs is texture evolution. It is known [5], that a study of the texture changes accompanying superplastic flow could elucidate the operating mechanisms. Perhaps the absence of these data is the reason why the origin of HSRS in MMCs is not yet clear. On the other hand, a complete study of structure evolution is required to predict service properties of MMCs subjected to superplastic deformation.

The aim of this paper is two-folds: first, to report new experimental results concerning microstructural and texture changes of the PM2014-20%Al_2O_3 during superplastic deformation composite; second, to examine physical mechanisms of superplasticity that are responsible for these changes. For these purposes the investigations of microstructure and texture evolution were carried out in conjunction with direct microstructural surface examination.

2. EXPERIMENTAL MATERIALS AND PROCEDURES.

The composite PM2014-20%Al_2O_3 was produced via a powder technology method from an aluminum alloy AA2014 (4.5%Cu, 0.6%Mg, 0.8%Mn, 0.8%Si, Al is the balance) and 20% particles

of Al_2O_3. For structure and texture analysis the tensile samples with the gauge section of 10x3x2 mm were machined from an extruded bar Ø16 mm in the longitudinal direction with respect to the original extrusion direction. For surface examination the samples were prepolished by a diamond paste (0.5μm), final polishing was performed using a 20% nitric acid solution in methanol at -30^{0}C and 15 V. Samples were deformed in tension in air at T=500^{0}C and at initial strain rates $8.3\cdot10^{-4}$, $3.3\cdot10^{-2}$ and $8.3\cdot10^{-2}$ s^{-1} to the fixed strains using a Schenck RMS-100 universal testing machine.

The metallographic analysis of deformed specimens was performed using an optical microscope Neophot-32, a JSM-840 and a structural analyzer Epiquant. The complete{111} pole figures were determined by X-ray measurements using a universal diffractometer DRON-4 and CuK_α radiation.

3. RESULTS.

3.1 Mechanical properties.

It was reported in prior works [6, 7] that this composite demonstrated superplastic behavior at T=500^{0}C in the range of high strain rates $\dot{\varepsilon}=10^{-2}$ -10^{-1} s^{-1}. The optimum strain rate of superplasticity is $\dot{\varepsilon}=1.6\cdot10^{-2}$ s^{-1}. At this strain rate the highest elongation-to-failure (δ=210%) and the maximum value of the coefficient of strain rate sensitivity (m=0.45) was arrived. In region I at $\dot{\varepsilon}=8.3\cdot10^{-4}$ s^{-1} (δ=112% and the m=0.2) and in region III at $\dot{\varepsilon}=8.3\cdot10^{-2}$ s^{-1} (δ=105% and the m=0.24) superplastic behavior was not established.

3.2 Microstructure evolution.

3.2.1 Initial structure.

The as-received state of the composite has an anisotropy distribution of alumina particles (Fig. 1a) [5]. Reinforced particles tend to align toward the extrusion direction. In this direction their average length is 6-8μm. In the transverse direction their shape is circular and their average size is about ≈ 2 μm. The distribution of particles is not completely uniform. Clusters of reinforced elements are observed in the composite. Grains of aluminum matrix are rather equiaxed and their average size is about 2.5 μm.

3.2.2 Microstructural evolution in region I.

In the early stage of plastic flow an extensive growth of matrix grains takes place (Table 1). The grains elongate toward the tension direction (Fig. 1b). The aspect ratio between longitudinal and transverse sizes of the matrix increases up to strain ε=100%.

Table 1. The influence of strain and strain rate on the matrix grain size (μm). Notice that, the nominator is the size in longitudinal direction and the denominator is one in transverse direction.

Strain, ε (%)	Strain rate, $\dot{\varepsilon}$ (s^{-1})		
	$8.3\cdot10^{-4}$	$3.3\cdot10^{-2}$	$8.3\cdot10^{-2}$
5	4.0/3.1	-	-
15	-	-	-
50	4.7/3.5	4.0/3.0	3.3/2.5
100	8.5/5.1	4.5/3.7	4.0/3.5

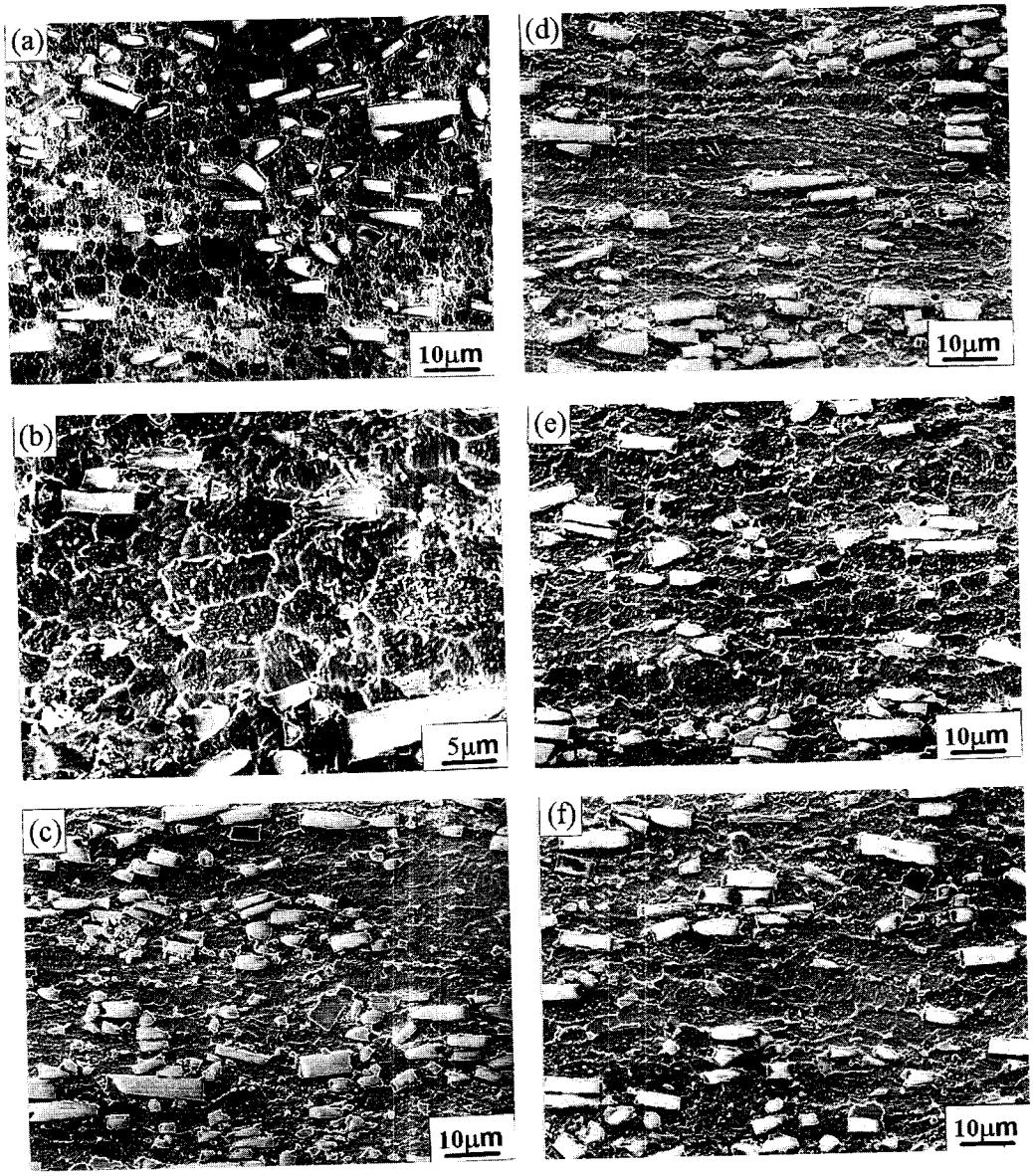

Figure 1. (a) Micrograph of the as-received state of the composite PM2014-20%Al_2O_3; Microstructures of the deformed composite at $T = 500^0$C: (b) $\dot{\varepsilon} = 8.3 \cdot 10^{-4}$ s^{-1}, ε=100%; $\dot{\varepsilon} = 3.3 \cdot 10^{-2}$ s^{-1}: (c) ε=15%, (d) ε=30%, (e) ε=50%, (f) ε=100%. (SEM)

3.2.2 Microstructural evolution in region II.

In region II in the early stage of plastic flow matrix grains grow and elongate toward the tension direction (Fig. 1c). Strain increase up to ε=30% yields formation of deformation bands located along tension direction (Fig. 1d). The length of deformation bands attains tens of microns and their width is determined by the distribution of particles at the site of specimen and constitutes about 2-8 μm. The

broadening of deformation bands and their volume fraction increases with strain increase up to ε=30%. After this strain two structural components can be distinguished in the composite microstructure. The first component is a banded structure. This structural component occupies approximately 60% of the material volume and locates in the particle-free areas. The second component is comprised of circular grains of about 5μm in size. This structure is observed in areas of reinforced element clusters. At further deformation a dynamic recrystallization occurs in the band structure. As a result, uniform granular structure forms in the whole volume of the composite at ε=50% (Fig. 1e). Following deformation up to strain ε=100% causes an essential growth of matrix grains (Fig. 1f).

3.2.3. Microstructural evolution in region III.

Plastic deformation in region III leads to a slight grain growth in the aluminum matrix and elongation of these grains toward the tension direction. Deformation bands do not form. A refinement of initial grains occurs, notably [6] at strain rates higher than $\varepsilon=10^{-1}$ s^{-1}.

3.3 Texture changes during deformation.

In the as-received state of the composite a rather weak <111> fibre texture was observed (Fig. 2a).

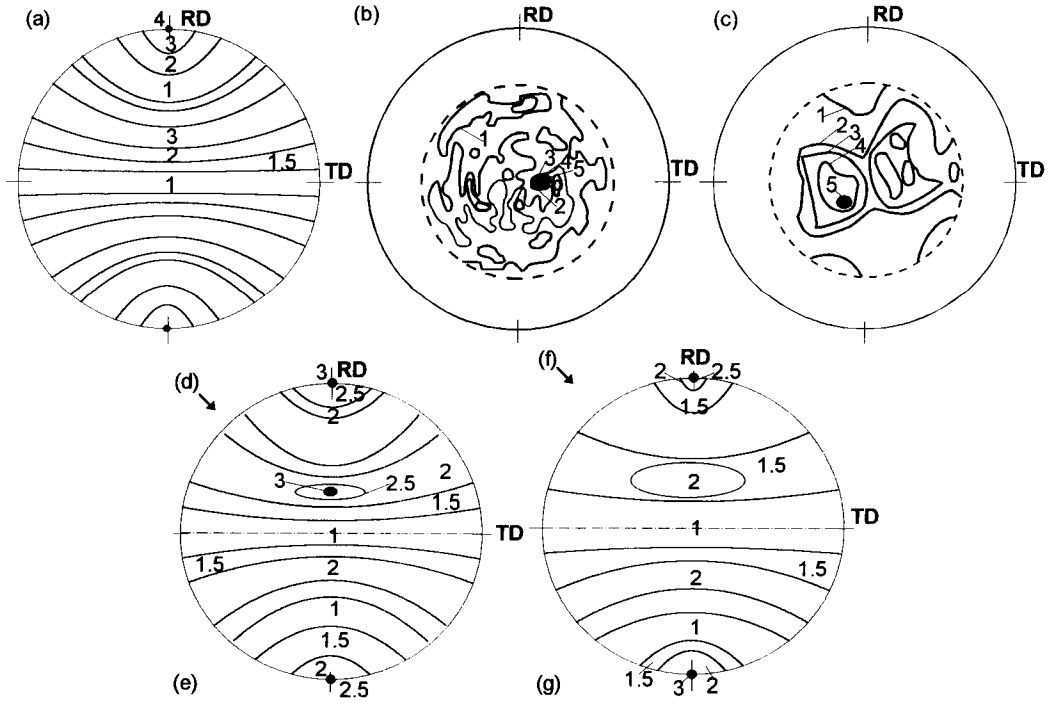

Figure 2. <111> pole figures for the composite PM2014-20%Al_2O_3 (a) the as- received state; after deformation at T=500°C $\dot{\varepsilon}=3.3\cdot10^{-2}$ s^{-1}: (b) ε=15%, (c) ε=30%, (d) ε=50%, (e) ε=100%; (f) $\dot{\varepsilon}=8.3\cdot10^{-4}$ s^{-1} ε=100%, (g) $\dot{\varepsilon}=8.3\cdot10^{-2}$ s^{-1} ε=100%.

Following isochronal annealing at T=500^{0}C negligibly influences texture intensity. Texture evolution during superplastic deformation in region II differs significantly from texture evolution both at lower strain rates and at higher strain rates. In region I plastic deformation leads to reduction of texture intensity in the initial stage of plastic flow. Further deformation up to strain ε=100% does not remarkable affect intensity and texture type (Fig. 2f). The texture is not random and the <111> type is retained.

In region II the overall texture decreases following superplastic deformation (Fig. 2b). Deformation up to strain ε=30% results in a break of the initial texture (Fig. 2c). Texture intensity sharply decreases and, it could be concluded, that the texture was rather random and close to <110> fibre texture. Strain increase up to ε=50% results in restoration of <111> fibre texture (Fig. 2d). Following deformation leads to formation of the right symmetric texture (Fig. 2e).

In region III the <111> fibre texture is seen (Fig. 2g). During plastic flow no significant changes in the texture were revealed.

3.4 Surface microstructural observations.

At all examined strain rates the grain groups slide as an entity [8-10]. The evidences of CGBS were revealed at all studied deformation conditions. However, the surface metallographic features were to be dependent on strain rates. The characteristic of matrix grains sliding in groups and the size of the grain groups is different in three strain rate ranges.

In region I two systems of CGBS is operative in the early stage of plastic flow (Fig. 3a). It is difficult to reveal a preliminary CGBS system. The shift of grain groups occurs along two systems of grain boundary surfaces oriented at an angle of ~60^0 to the tensile axis. As a result, the grain groups are equiaxed. The surfaces of CGBS are not planer. The surface bending is observed in the sites of intersection of the surfaces and reinforced particle. The sliding grain groups shift as a unit along common grain boundary surfaces. They are located in the areas of reinforcements clusters. Their size is about 2-4 in units of average matrix grain size. Strain increase leads to reduction of the grain group size up to 2. The same tendency was found in monolithic alloys [8, 9].

In region II only one system of CGBS is observed at a small strain (Fig. 3b). The stringers of deformation bands of this system are continuous and oriented at an angle of ~70^0 to the tensile axis. Their length is about 20-50 μm. The spacing between these bands is about 3-4 in units of average matrix grain size. The grain groups have a right-angle shape. In general, the shift of longitudinal scratches is observed. However, it is seen from Fig. 3b that there are no shifts of some scratches on grain boundaries although the strain is basically accumulated due to CGBS [8]. It was shown [8] that not only the scratch shift but also the breakage of these scratches indicates to contribution of GBS to the total deformation

Notice that formation of continuous CGBS surfaces occurs as a result of sliding along intergranular boundaries. Interfacial sliding was not observed. Evidence of CGBS is observed in the vicinity of the particles only in the case when the Al_2O_3 is located on a Al/Al boundary. An increase in strain up to ε=40% leads to a decrease in spacing up to about 3 (Fig. 3c). In macroscale the bands form stringers, which traverse the specimens from one edge to the other. Notice that the stringers are rather discontinuous. In addition, in some areas of the tested sample evidence of the secondary CGBS system is detected. However, their amount is insignificant in comparison with traces of the primary CGBS system.

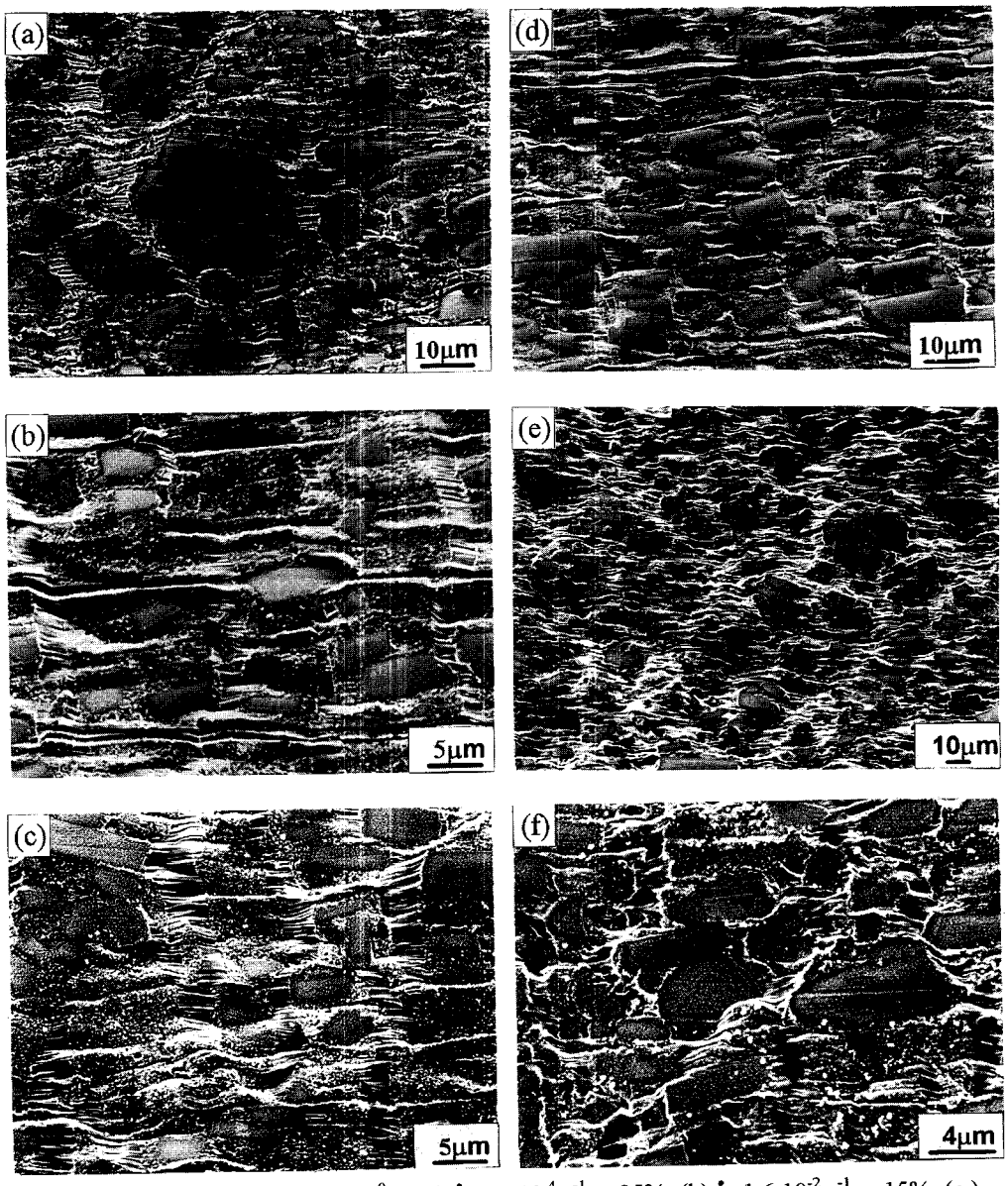

Figure 3. Deformation relief at T=500^{0}C: (a) $\dot{\varepsilon}$=8.3·10^{-4} s^{-1} ε=25%; (b) $\dot{\varepsilon}$=1.6·10^{-2} s^{-1} ε=15%, (c) ε=40%, (d) and (e) ε=80%; (f) $\dot{\varepsilon}$=1.6·10^{-1} s^{-1} ε=20%. Note that the tensile axis is horizontal.

Further strain up to ε=80% leads to a strong reduction of the spacing up to 1-2 and a significant increase in broadening of deformation bands (Fig. 3d). The primary system of CGBS is a dominant. Evidence of secondary CGBS system operation was rarely observed. As usual, GBS occurs along common surfaces consisting of grain boundaries of different grain groups. These surfaces are not flat and there is surface irregulation in the sites of transition from one grain group to another.

In region III GBS is also operative (Fig. 3f). However, the degree of cooperation of GBS is much less. It is rather difficult to recognize the stringers of CGBS. One system of CGBS prevails. The spacing between these stringers is 1-2 in units of average grain size. In general, GBS of individual matrix grains takes place. The mutual sliding and rotation of grains along stringers of CGBS is well revealed while sliding along individual intergranular grain boundaries can be detected only by the scratch shift. The intensity of GBS at high strain rates is less than at low strain rates. This is caused by the fact that the contribution of dislocation glide to total deformation is a dominant [3]. This is evident from reduction in spacing between parallel longitudinal scratches. Consequently, the contribution of GBS to the total elongation is not high.

4. DISCUSSION.

4.1 Operating deformation mechanisms.

It was shown in prior works [6, 7] that the deformation of the PM2014-20%Al_2O_3 composite is controlled by deformation in the aluminum matrix. The gap between deformation behaviors of the composite and its monolithic alloy is associated with the influence of reinforced elements on deformation mechanisms in the aluminum matrix [7]. It is generally known [3] that in monolithic alloys GBS is the dominant deformation mechanism in region II. However the contribution of GBS to the total elongation decreases in region I and III. The conducted experiments show that in the case of the composite the situation is the same. The occurrence of extensive GBS is evident from direct surface microstructural examination and consistent with an experimental value of m=0.45 in region II [3, 7].

At the same time the character of CGBS is not typical for conventional superplasticity [8-10]. At the optimum strain rate of superplastic deformation the secondary system of CGBS begins to act only after large strain. In addition, the size of grain groups is significantly less than in monolithic aluminum alloys [8-11]. Probably, the later causes a shift of region II toward higher strain rates in the composite as compared to the monolithic alloys.

4.2 Deformation mechanisms and structural evolution.

It is known [3, 7, 12] that dynamic changes in grain size and texture evolution are caused by operation of different modes of deformation during superplastic flow. Accordingly, unusual structure and texture evolution observed in the composite during superplastic deformation can be explained in terms of dominant deformation mechanisms.

In region I multiple CGBS and single dislocation glide are the main deformation mechanisms [3, 6]. As a result, the <111> initial fibre texture is preserved during deformation and its randomization is observed. Lattice dislocations are trapped by matrix grain boundaries during plastic deformation [6]. Sliding along grain boundary surfaces results in adsorption of trapped dislocations by matrix grain boundaries [3]. This leads to increase of grain boundary energy and provides extensive grain growth due to deformation induced grain boundary migration coupling with CGBS. At the same time GBS does not occur along boundaries in the grain group interior. Dislocation sliding in these "internal" grains yields their elongation toward the tension direction. In addition, accumulation of lattice dislocations inside these grains and into their boundaries takes place in the initial stage of plastic flow [6]. As strain increases the average size of grain groups drops. GBS becomes more uniform and occurs along most of the matrix boundaries. As a result, a reduction in lattice dislocation density takes place [6].

In region II single CGBS leads to a great shift of the grain groups in the aluminum matrix. Most likely, this shift is accommodated by single slip [3]. Operation of these two deformation mechanisms yields microstructural band appearance in the reinforced particle-free areas. The details of formation of these bands are not yet clear. However, it is possible to presume that this process occurs due to the coalescence of matrix grains inside of the grain groups and deformation induced migration of transverse boundaries of the grain groups. It is known [8], an extensive grain growth takes place in bands of CGBS in monolithic alloys. In any case, band formation leads to disappearance of the initial texture and formation of the non-symmetric one after ε=15%. Dislocation density sharply increases in coarse deformation bands [6]. Dislocation accumulation inside of the bands provides critical conditions for dynamic recrystallization occurrence. This leads to formation of fine equiaxed grains. CGBS takes place along their boundaries. As a result, after large strain the CGBS becomes more uniform. Mutual sliding of matrix grains provides the best conditions for adsorption of trapped lattice dislocations into grain boundaries. This yields the significant reduction of lattice dislocation density [6].

In region III the dominant multiple slip provides the stabilization of initial <111> fibre texture and results in elongation of matrix grains toward the tension direction. Slight weakening of texture intensity is caused by GBS which is operative at a level of individual grains. The velocity of adsorption of grain boundary dislocations due to GBS is less than that of lattice dislocation generation. As a result, plastic deformation leads to an increase in dislocation density [6].

5. REFERENCES.

[1] T. G. Nieh and J. Wadsworth, Mat. Sci. and Eng. **A147,** 129 (1991).
[2] R. S. Mishra, T. R. Bieler and A. K Mukherjee, Acta. Metall. Mater. **43,** 893 (1995).
[3] O. A. Kaibyshev, Superplasticity of Alloys, Intermetallides, and Ceramics (Berlin, Springer-Verlag,), 316 (1992).
[4] K. Higashi, T. G. Nieh, M. Mabuchi and J.Wadsworth, Scr. Metall. Mater. **32,** 1079 (1995).
[5] A. Padmanabhan and K. Lucke, Z. Metallkde 77, 765 (1986).
[6] R. Kaibyshev, V. Kazykhanov, E. Evangelista and J. Stobrawa, Mater. Sci. Forum **170-172,** 525 (1994).
[7] R. Kaibyshev, V.Kazykhanov, V. Astanin and E. Evangelista, Mater. Sci. Forum **170-172,** 531 (1994).
[8] M. G. Zelin, N. A. Krasilnikov, R. Z. Valiev, M. W. Grabski, H. S. Yang and A. K. Mukherjee, Acta Metall. Mater. **42,** 119 (1994).
[9] M. G. Zelin and A. K. Mukherjee, Acta Metall. Mater. **43,** 2359 (1995).
[10] V.V.Astanin, O.A.Kaibyshev, S.N.Faizova, Acta.Metall.Mater. **42** 2617 (1994).
[11] I.I.Novikov, V.K.Portnoy, V.M.Iljenko, V.S.Levchenko, Superpl. in Adv. Mater. ed. S.Hori, M. Tokizane, N. Furushiro, 121 (1991).
[12]. A. K. Ghosh and R. Raj, Acta Metall. **29,** 607 (1981).

Ceramic and Metal Matrix Composites
doi:10.4028/www.scientific.net/KEM.127-131

Structure and Texture Evolution of the Metal Matrix Composite PM2014 Al-20%Al₂O₃ during Superplastic Deformation
doi:10.4028/www.scientific.net/KEM.127-131.961